

Combined gravity and magnetic studies of satellite bodies associated with the giant Coompana negative magnetic anomaly in South Australia

Clive Foss*

CSIRO Mineral Resources
North Ryde, NSW
Clive.foss@csiro.au

Philip Heath

GSSA
Adelaide, SA
Philip.Heath@sa.gov.au

Tom Wise

GSSA
Adelaide, SA
Tom.Wise@sa.gov.au

Rian Dutch

GSSA
Adelaide, SA
Rian.Dutch@sa.gov.au

SUMMARY

We present inversion models derived for 3 gravity and magnetic anomaly pairs. These anomalies are associated with the much larger (>50 km diameter) Coompana negative magnetic anomaly, and are due to high density and strong, reverse remanent magnetization. Recent drilling has revealed gabbroic rocks are likely to be the principal causes of these anomalies. In some cases the gravity and magnetic anomaly models are quite similar to each other, and from these we mostly gain estimates of the magnetization to density relationships. In particular, these cases confirm that the magnetization direction estimates derived from inversion of the magnetic field data are robust. In other cases the gravity and magnetic inversion models differ significantly, revealing that the simple models derived from inversion of either dataset alone do not well represent what is clearly a more complex geology. The main advantage from the combined gravity and magnetic data is to compare the information each separately provides. We hope to upgrade our inversion models with physical property values measured on core recovered from the recently drilling campaign. At that time, and in conjunction with petrological studies, we should be able to introduce more geological interpretation and guidance to modify and transform the initial inversion results which are primarily geophysical to models that are more geological.

Key words: Coompana Reverse Remanent Magnetization Density Gravity Magnetic Anomaly Gabbro

INTRODUCTION

As part of the PACE Copper exploration initiative the Geological Survey of South Australia has acquired new aeromagnetic and ground gravity data over the Coompana Area in the southwest of the state. The aeromagnetic data was acquired at 200 and 400 metre line spacing and 60 metres elevation above ground surface, and the gravity data was acquired at between 500 metres and 2 km spacing (on a grid designed following the results of the earlier magnetic mapping). Images of Bouguer Gravity and Total Magnetic Intensity (TMI) of the region including the major Coompana negative magnetic anomaly are shown in Figure 1. In this paper we investigate several of the sharp anomalies which appear in both the magnetic and gravity data (in areas 'A', 'B' and 'C' in Figure 1).

The magnetic field anomalies are clearly due to a predominantly reverse remanent magnetization which can be reliably addressed with suitable inversion procedures, causing no substantial increase in uncertainty of the results beyond those for inversions of equivalent anomalies dominated by induced magnetization. If we believe that both the gravity and magnetic anomalies are due to a single lithology with consistent ratio between its density and magnetization contrasts against the surrounding rocks then we are justified in applying a joint inversion to find (with some appointed weighting function) the optimum model which best matches both data sets. However, where there is a substantial discordance between the best-fit gravity and best-fit magnetic models, the imposition of a constant relationship between density and magnetization is likely to be invalid. This is the general case where geology is complex, with different relationships of various lithological units to density and magnetization distributions. A magnetic anomaly arises purely from ferromagnetic minerals, which even for the strongly magnetized rocks generating the prominent magnetic anomalies at Coompana are unlikely to constitute more than a few percent of the rock mass. This is too little to have a substantial effect on the density of the rock, so any relationship between density and magnetization is mostly through their association with a common lithology. Borehole intersections with what are believed to be sources of the gravity and magnetic anomalies were made only shortly before the writing of this abstract, at which time no density or magnetization measurements had been made, but the main recovered material from what are believed to be sources of the anomalies is gabbroic (as had been anticipated from the combined positive gravity and strong negative anomalies). Gabbroic bodies (including layered systems) can have complex distributions of density, particularly if they include ultrabasics and/or anorthosites, and also substantial contrasts in magnetization where different phases have variable iron:titanium ratios or ferromagnetic mineral content. Relationships between magnetization and density between different units in a mafic or ultramafic complex are poorly predictable, but fortunately physical property measurements on the recovered core should provide valuable constraints with which to upgrade our initial inversion models, although those constraints from the sparse drilling are likely to still leave considerable uncertainties in constructing inversion models and interpreting their results.

Figure 2 shows the location of stations in the western section of the Coompana gravity survey, which was designed to provide high resolution over areas in which we knew there were strong near-surface magnetizations. Figure 2 also shows the vertical derivative of gravity which has a closer match to the TMI for the sharper (shallower-sourced) features of interest than does the original Bouguer Gravity image. The anomalies of interest are negative in the TMI data (interpreted as due to reverse remanent magnetization) and

positive in the gravity data (interpreted to indicate dense, probably basic or ultrabasic lithologies). The property contrasts giving rise to the sharp gravity and magnetic anomalies are assumed to be at or close to the top of basement, which in this area is mostly at depths estimated to be in excess of 200 metres. For anomalies in areas A and B there is little or no justification for modelling the simple gravity and magnetic anomalies with anything other than a homogeneous contrast in the relevant physical property. However, inversion of both the gravity and magnetic data may require more complex models to reconcile the two separate, simple models derived from each dataset alone. The anomaly in Area C provides an example where the magnetic field study has already established that there is a complex distribution of inhomogeneous magnetization. These case studies of progression from single-property to dual-property models highlight the value of combined constraints of two independent data sets sensitive to different physical properties.

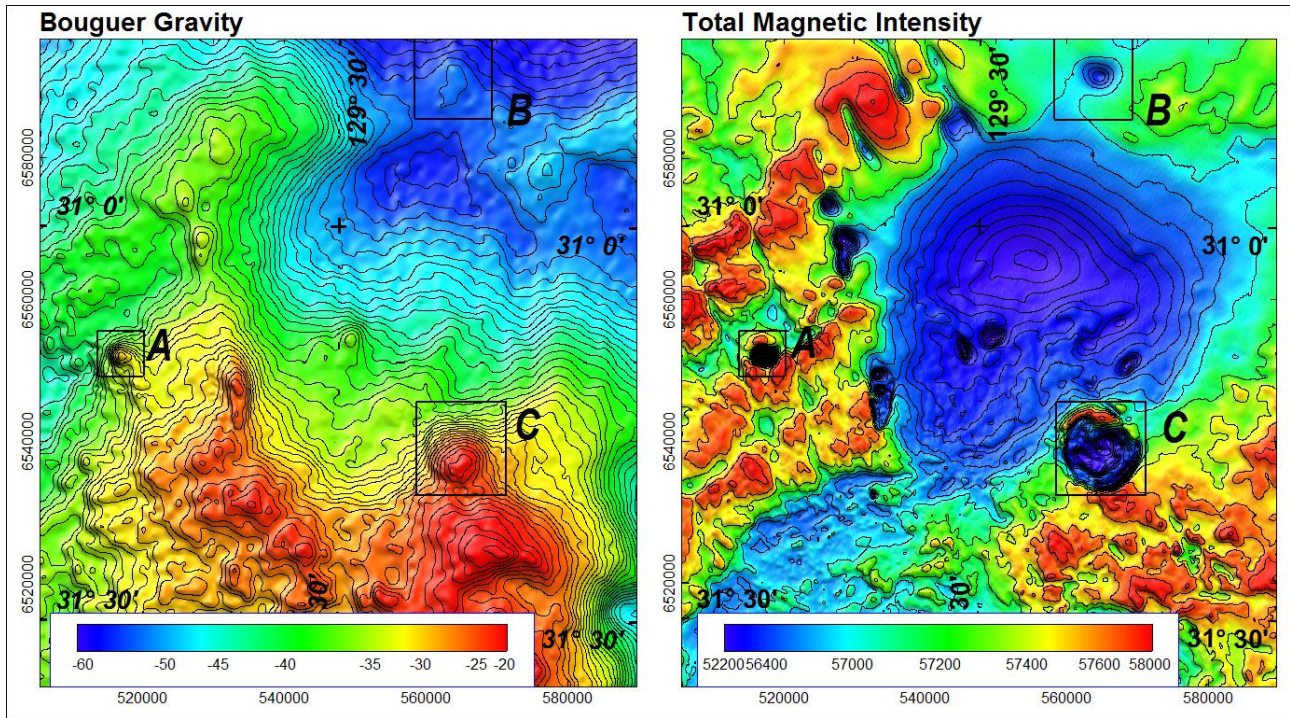


Figure 1 (left) Bouguer Gravity and (right) Total Magnetic Intensity

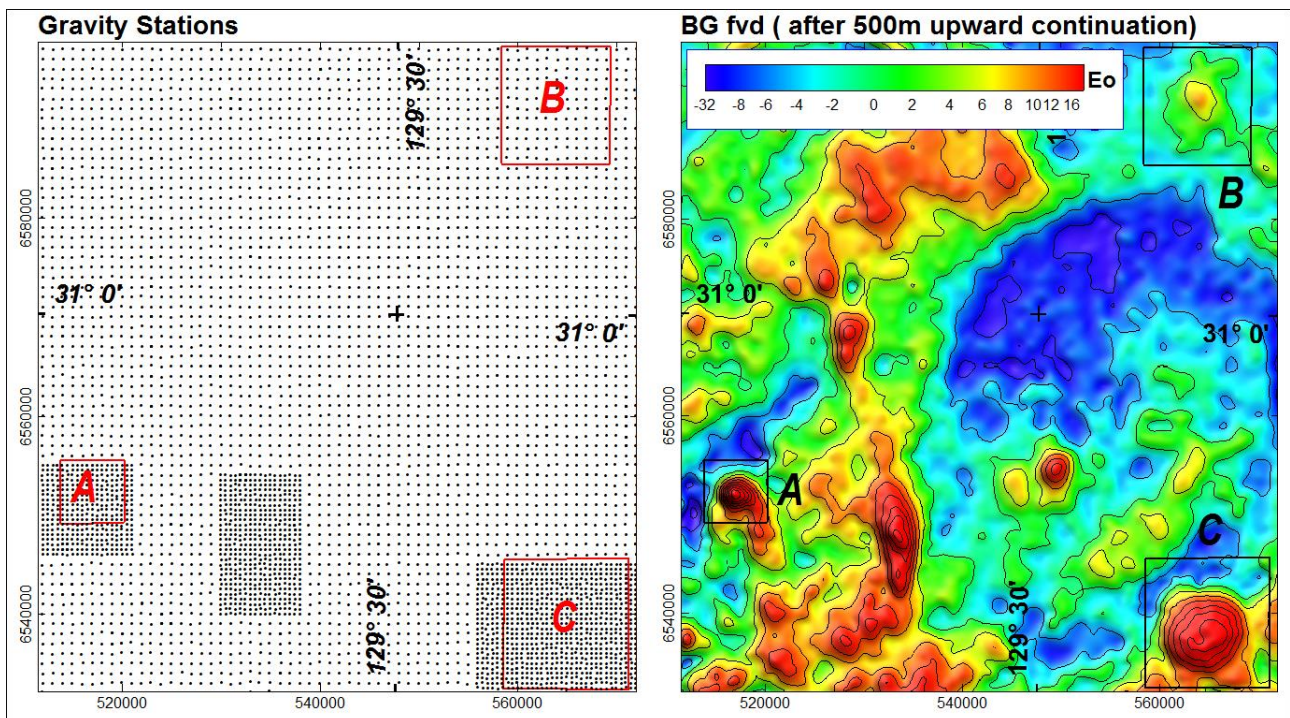


Figure 2 (left) distribution of gravity stations and (right) vertical derivative of 500 metre upward continued Bouguer Gravity.

ANOMALY A

Figure 3 shows the Bouguer gravity and TMI anomalies in Area A. There is a strong spatial correlation between the anomalies suggesting that they are due to a common source. The gravity anomaly is superimposed on a strong regional gradient. The magnetic anomaly includes a slight complexity (revealed by local distortion of the otherwise smooth contours) suggesting a local, more intense magnetization towards the top of the source body. Figure 4 shows a perspective of alternative ellipsoid and elliptic pipe models which both match the gravity anomaly, and similarly two alternative models to match the magnetic anomaly. Also shown is a small, shallow magnetic source model developed to explain the local irregularities in the contours at the centre of the magnetic anomaly. This small source is significant as it provides the best available constraint on depth to the top of the magnetization. The larger homogeneous density and magnetization inversion models closely match the measured fields. These inversion body volumes are best considered as approximate bounds within which there are what are likely to be variable property distributions (but with mean values similar to those of the homogeneous models).

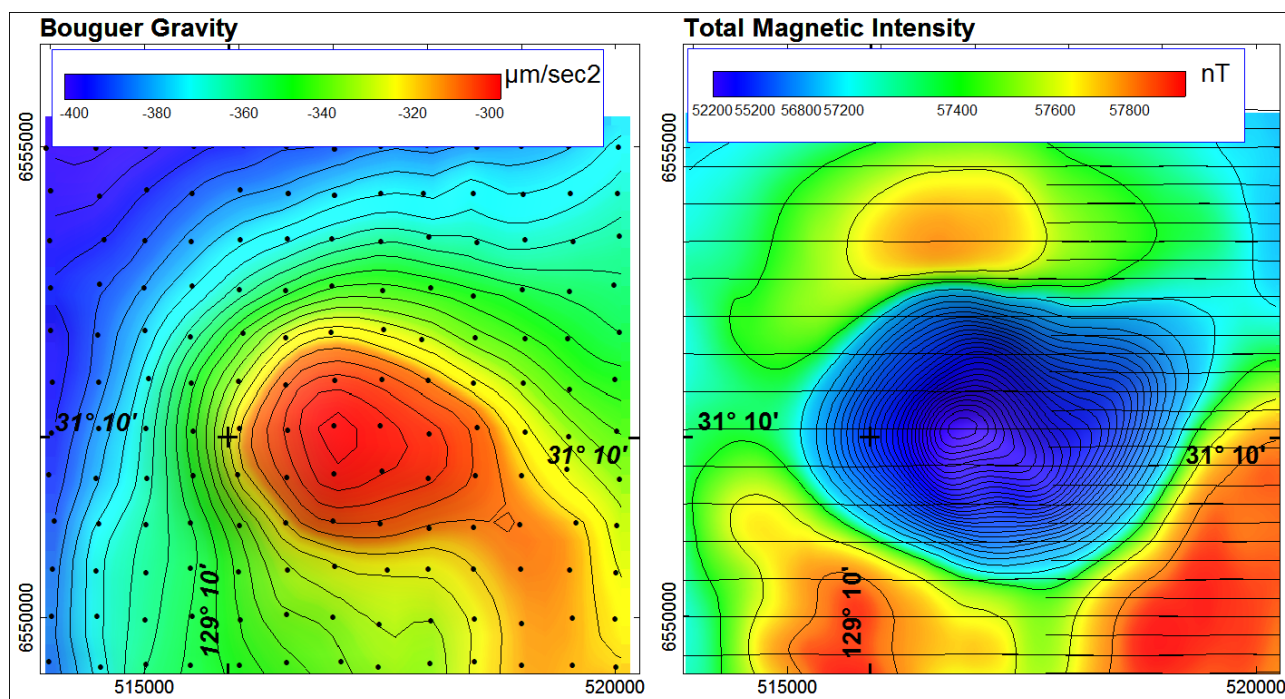


Figure 3 (left) Bouguer gravity and (right) Total Magnetic Intensity anomalies in Area A.

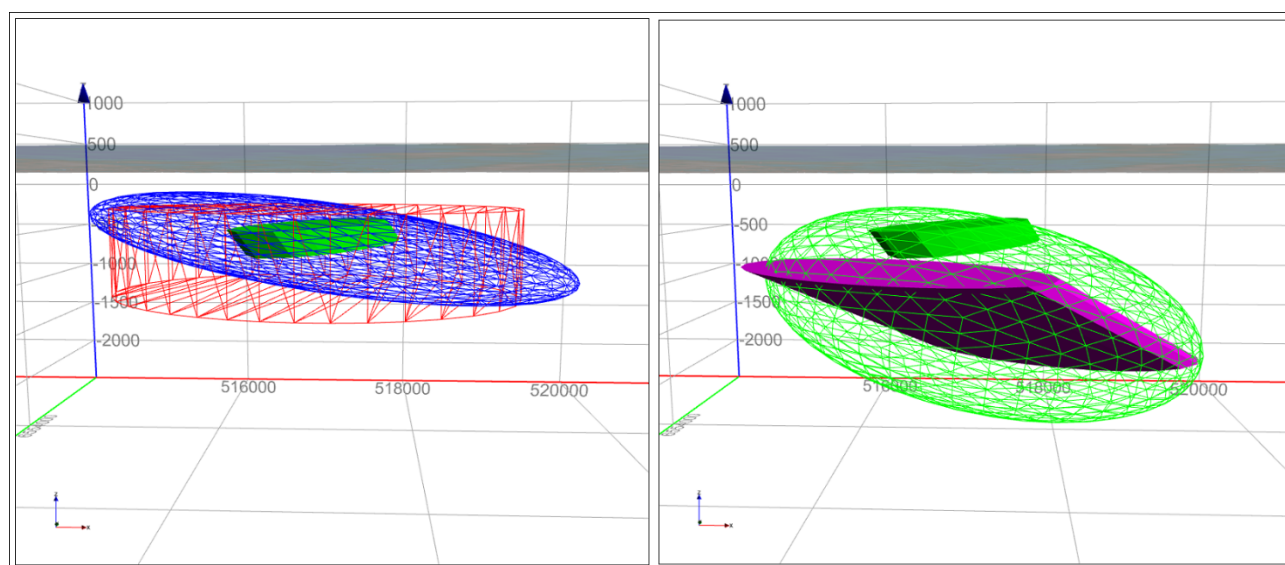


Figure 4 (left) alternative gravity models (red and blue) with shallow magnetic model shown for reference. (right) magnetic models (purple and green net) with (green) a model of more intense shallow magnetization.

The horizontal centres and extents of the gravity and magnetic models as shown in Figure 4 are very similar, with the major differences between the models in their depths and depth extents. Figure 5 shows gravity and magnetic fields computed from the magnetic and gravity models, each switched to explain the other field, using best-fit properties found

by single parameter inversion. The magnetic model produces a match to the gravity field almost as good as the dedicated gravity inversion model, so that body explains the variation in both fields. This gives us an estimate of the relationship between density-contrast and magnetization-contrast, but does little to improve the spatial constraint of the model, with considerable uncertainty remaining about its depth. As also shown in Figure 5, the gravity model generates a reasonable match to the magnetic field (but less acceptable than the fit of the magnetic model to the gravity field). The magnetic field inversions require simultaneous estimation of magnetization direction and spatial parameters. The full magnetic field inversion returned an estimated magnetization direction of declination 354° , inclination $+52^\circ$. The inversion using the gravity model gave estimates of declination 345° , inclination $+51^\circ$, less than 6° different, illustrating that estimation of magnetization direction from this anomaly is robust. We don't know the density of the surrounding rocks, but based on pre-drilling geological interpretation (Wise et al., 2015) we expect those densities to be close to 2750 kg/m^3 (we hope to upgrade this estimate with measurements on material recovered from the current drilling program). The ellipsoid gravity inversion model has a volume of 2.69 km^3 and a density contrast of 410 kg/m^3 , and the ellipsoid magnetic inversion model has a volume of 6.78 km^3 , and a density contrast of 220 kg/m^3 (the larger estimated total mass of the magnetic inversion model is because it is mostly deeper). The density estimate for both bodies of 3160 and 2970 kg/m^3 respectively are both feasible.

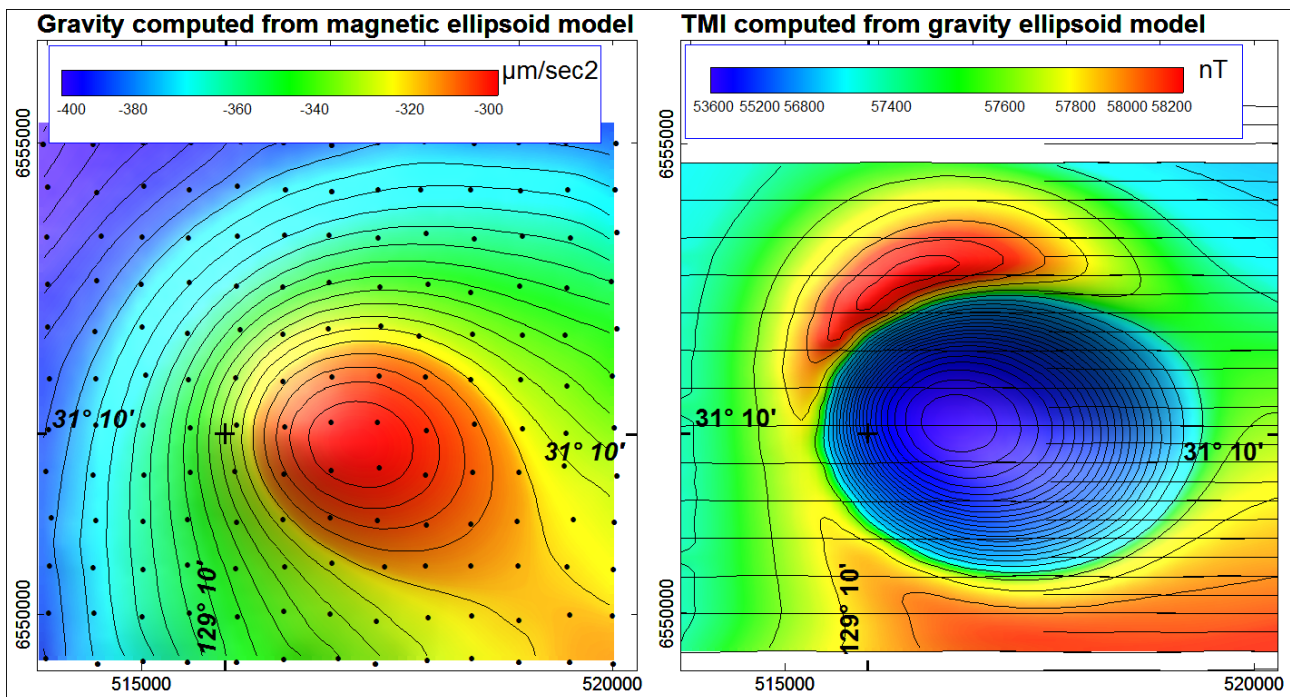


Figure 5 (left) Gravity computed from the magnetic ellipsoid model using a best-fit density. (right) TMI computed from the gravity ellipsoid model using a best-fit magnetization.

ANOMALY B

The anomaly pair in area B to the north of the main Coompana magnetic anomaly are shown in Figure 6. As in area A, the magnetic anomaly is predominantly negative due to reverse remanent magnetization. The gravity anomaly is more poorly defined than in area A, and its separation from the background field is more interpretive, mostly due to greater irregularity in the density distribution, but also in part due to the sparser gravity measurements in this area. The gravity and magnetic fields forward computed from the dedicated gravity and magnetic field inversions are shown in Figure 7. The magnetic field is a good fit to the measured data imaged in Figure 6, but the smoothness of the anomaly reveals that there are no tight constraints on the magnetization distribution (mostly due to the considerable estimated depth of burial). The computed gravity does not match the measured gravity as closely as in area A because (for reasons listed above) the gravity anomaly is less well suited to inversion. There is also a much poorer spatial correlation between the gravity and magnetic anomalies in area B compared to area A. This is highlighted in Figure 8, where there is a displacement of over 800 metres between the peak of the vertical derivative of Bouguer gravity to the northwest, and the peak of the total gradient (analytic signal) of TMI to the southeast. Both fields were upward continued by 500 metres before applying the various enhancements. For the gravity field this is to reduce artefacts arising from the influence of individual station positions in the gridding, and for the magnetic field it is to subdue the expression of near-surface magnetizations. The peaks in both data enhancements are expected to approximately mark the locations of the centres of anomalous mass and anomalous magnetization respectively, and their 800 m separation suggests that the two property distributions are not completely correlated. The residual gravity field generated by subtraction of a 2nd order polynomial surface before modelling is also imaged in Figure 8. The residual contours are very similar in pattern to the vertical derivative contours (suggesting that modelling the vertical derivative would be an alternative way of reducing the influence of the strong regional field variation). The circular model outline clearly does not well match the broader and more irregular outline of the residual anomaly. There appears to be a double step reduction from the anomaly peak to the background field, which suggests the

modelled anomalous density may be surrounded by another deeper, more diffuse or thinner zone of anomalous density too indistinct to reliably invert or model (it could be easily inverted, but there would be almost no confidence in the resulting model).

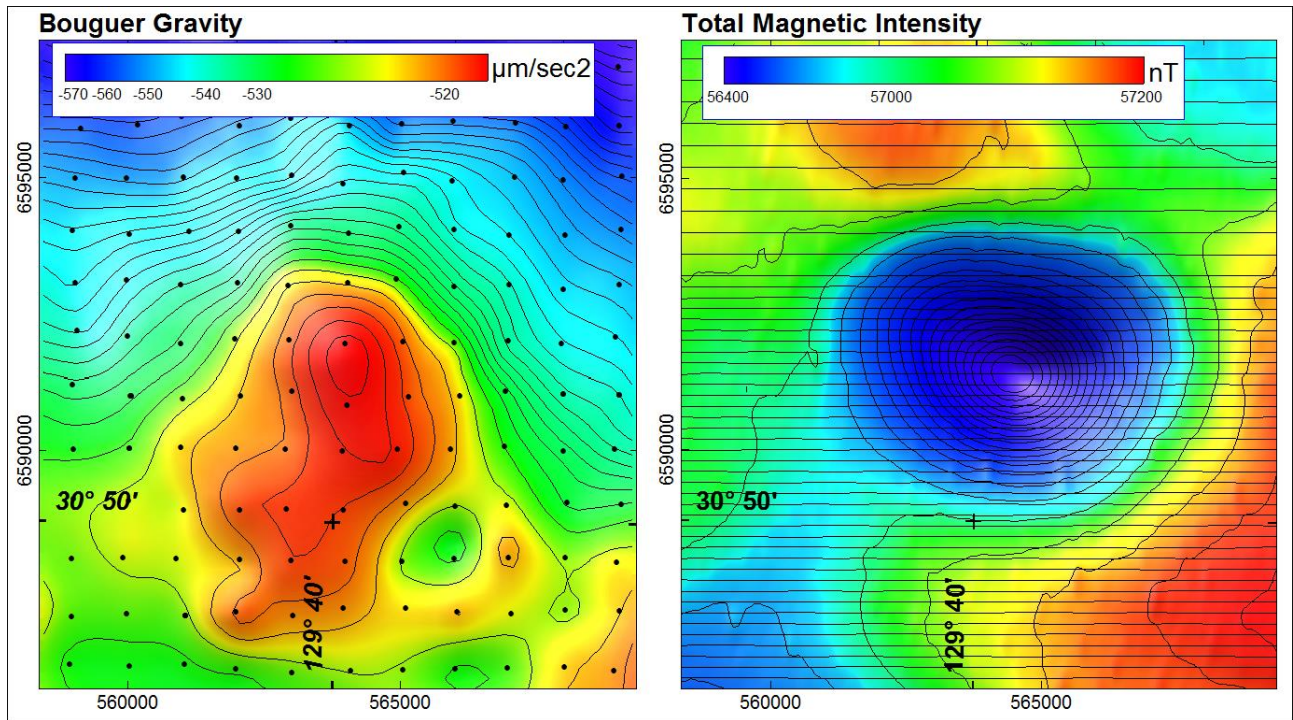


Figure 6 (left) Bouguer Gravity and (right) Total Magnetic intensity anomalies in Area B.

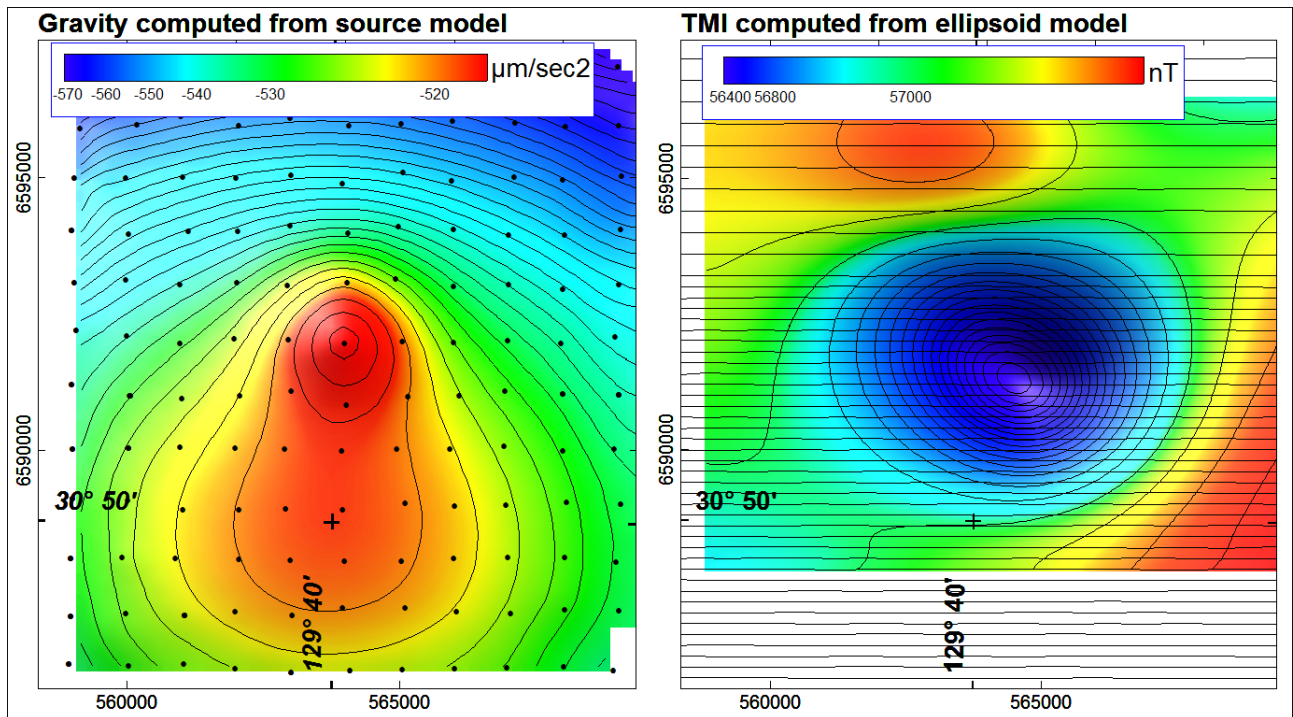


Figure 7 (left) Bouguer gravity forward computed from the gravity inversion model and (right) TMI forward computed from the ellipsoid magnetic field inversion model.

Figure 9 shows perspective views of alternative vertical circular pipe and vertical ellipsoid gravity inversion models, and also three alternative magnetic field inversion models. The two gravity models are both co-centred beneath the peak anomalous density mapped by the residual gravity anomaly. The three magnetic field inversion models are also co-centred but are off-centred from the gravity models. The 3 magnetic field inversion models produce almost identical estimates of magnetization direction. All three have very similar magnetic moments (the product of magnetization intensity and volume) but the poorly constrained individual volume and magnetization intensity values vary considerably between the models. The geological source giving rise to the gravity and magnetic anomalies in area B appears to have a compact zone of high density surrounded by more diffuse anomalous density and by a more

extensive and off-centred distribution of (predominantly remanent) magnetization. The apparent smooth and homogeneous distribution of magnetization may well be mostly due to its increased depth, which reduces the signature of any local internal variations.

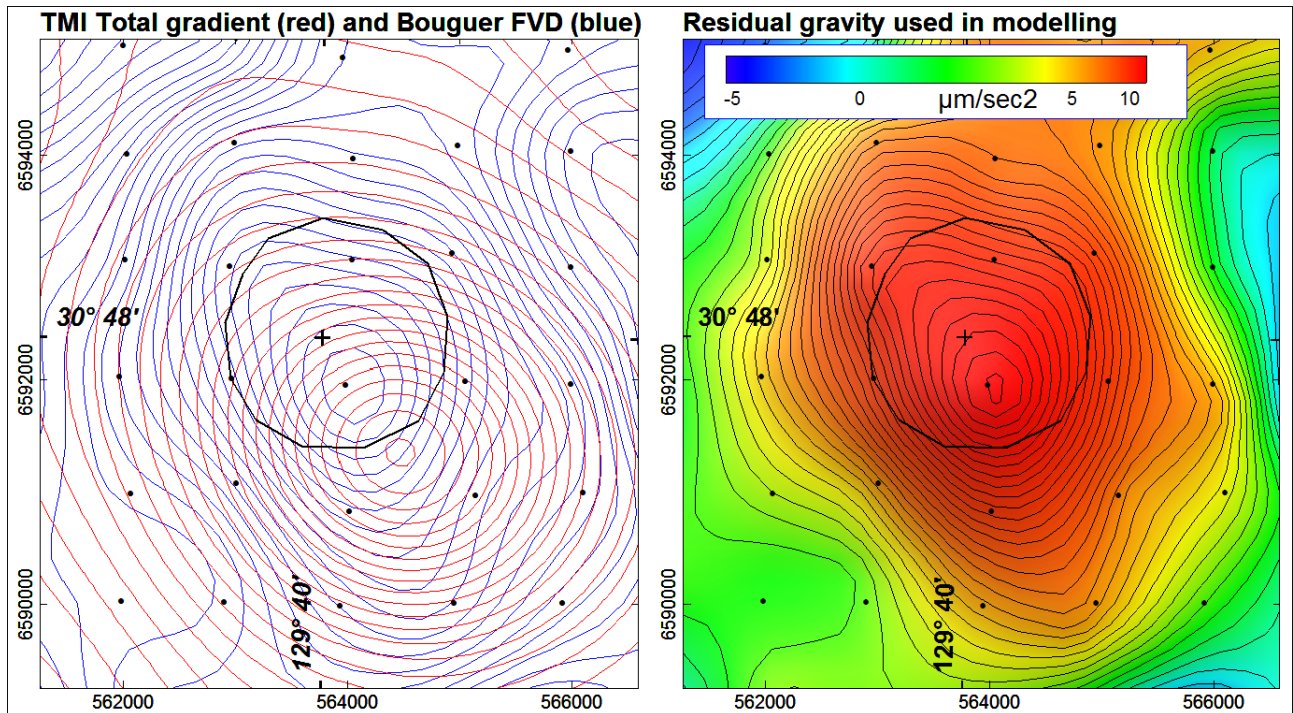


Figure 8 (left) contours of the vertical derivative of Bouguer gravity (after 500m upward continuation) - red, and of the total gradient of TMI (also after 500 metre upward continuation) - blue, and (right) residual Bouguer gravity after subtraction of a 2nd order polynomial background. The central circle is the outline of the circular pipe gravity model.

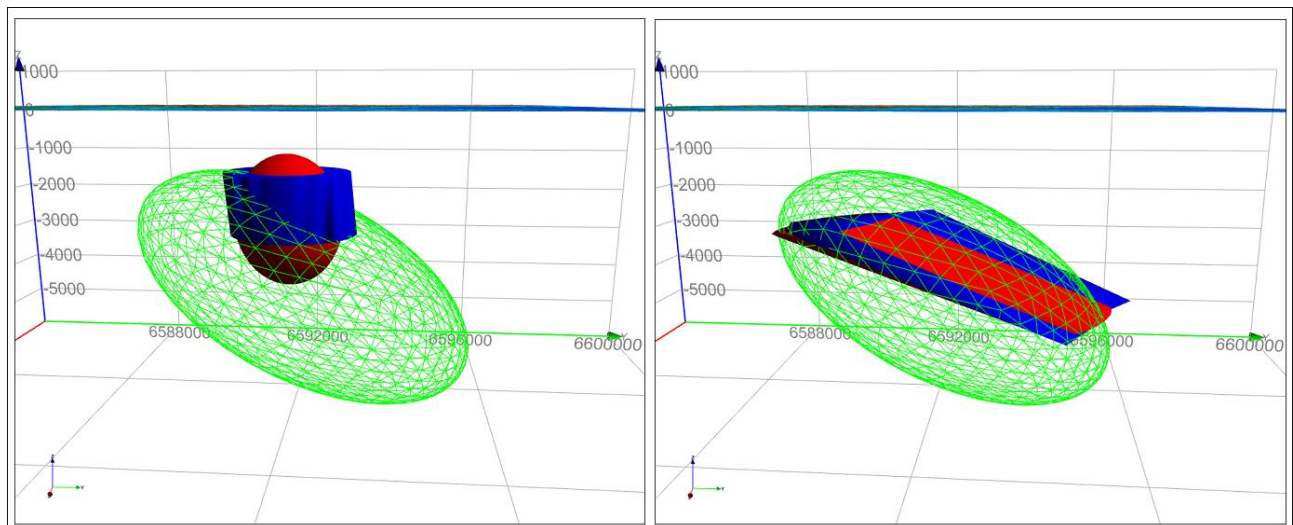


Figure 9 (left) alternative circular pipe (blue) and vertical ellipsoid (red) gravity inversion models with the ellipsoid magnetic inversion (green net) for reference, and (right) alternative ellipsoid, plunging elliptic and polygonal pipe magnetic inversion models.

ANOMALY C

Gravity and magnetic field variations in area 'C' to the southeast of the main Coompana anomaly are imaged in Figure 10. The gravity field shows a simple, circular positive anomaly. The magnetic anomaly is also broadly circular, but is complex and not co-centred with the gravity anomaly. As shown in Figure 11, the gravity anomaly is well matched by the field of a horizontal near-circular ellipsoid or a wide horizontal near-circular sheet. Matching the magnetic anomaly requires several different bodies, but this is well within the capabilities of an inversion, as illustrated by the image of the magnetic field forward computed from the magnetic field inversion model in Figure 11. The model consists of a pair of arcuate bodies around the southeastern and northern edge of the anomaly with strong reverse and normal magnetizations respectively, and inside that ring an outer sheet of reverse magnetization, and a superimposed inner sheet of more intense reverse magnetization. The edges of the outer and inner sheets are expressed as steps in the magnetic field anomaly. The inversion model reproduces all of the major features of the observed anomaly, but not all of the detail. In particular there

are several local features (some of which may possibly be feeder zones), but those require dedicated local inversions because they contribute such a small proportion of the anomaly that they are poorly constrained in a full-anomaly inversion (Foss et al., 2016).

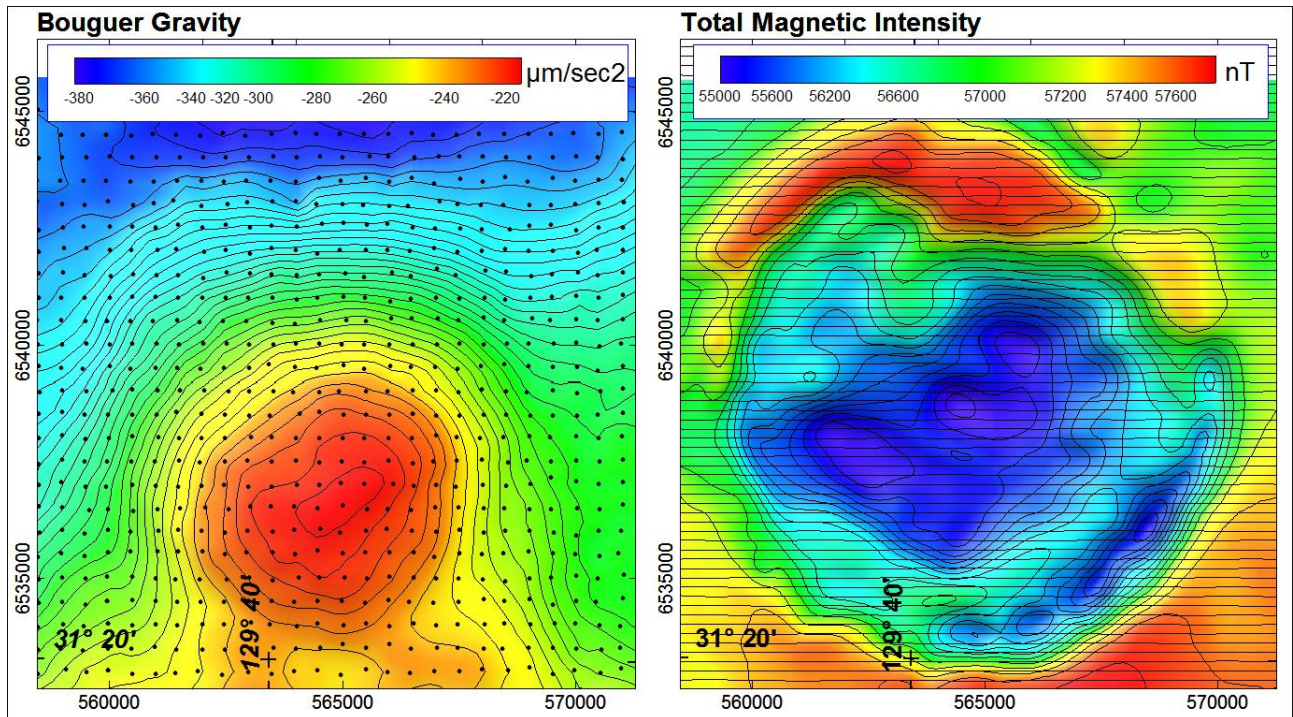


Figure 10 (left) Bouguer gravity and (right) TMI in area C.

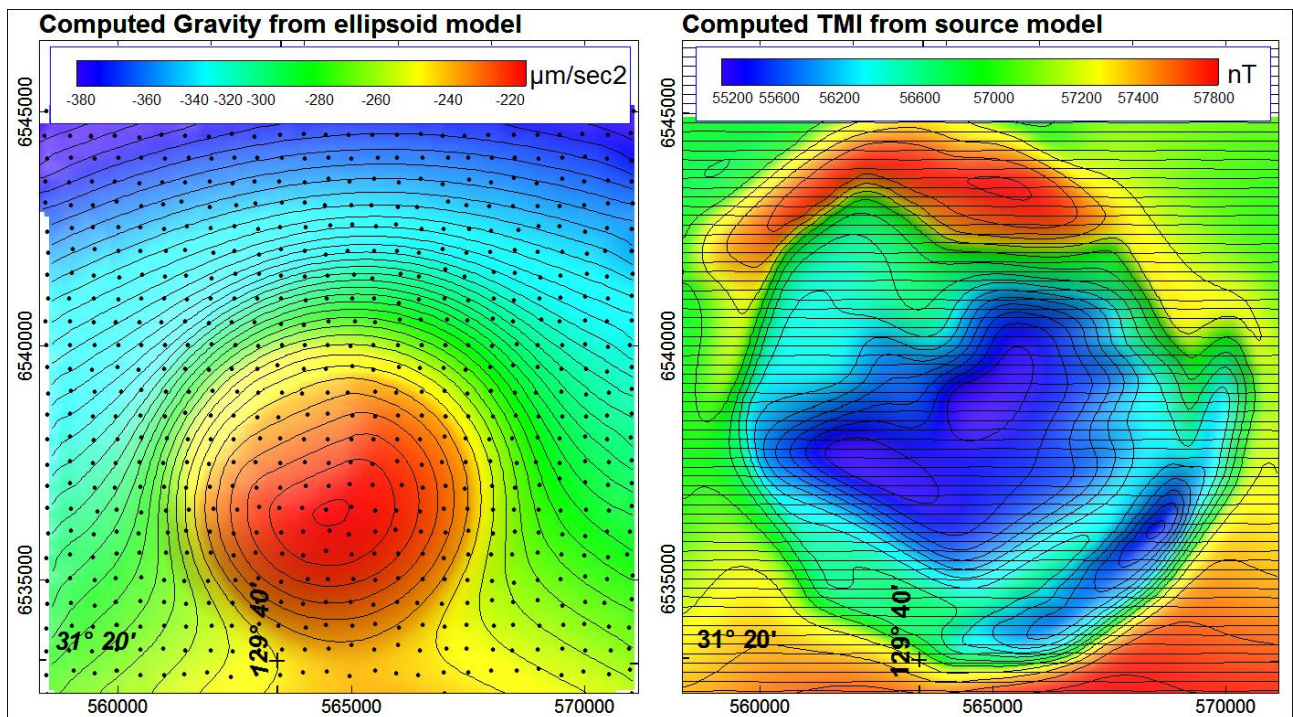


Figure 11 (left) Computed gravity from the elliptic sheet gravity inversion model, and (right) computed TMI from the magnetic field inversion model.

The gravity inversion model and the inner sheet of the magnetic field inversion model overlap quite closely, and the gravity anomaly can be well matched by assigning a suitable density to the inner sheet of the magnetic field inversion model. The gravity inversion model sheet has a thickness of 1400 metres and density contrast of 170 kg/m³. The magnetic field inversion inner sheet model has a thickness of 637 metres and a density contrast of 440 kg/m³, so that the two bodies have similar anomalous density-contrast thickness products and similar total anomalous densities. The estimated density values are 2900 kg/m³ and 3200 kg/m³ respectively. These wide

sheets are poorly suited to estimating depth-to-top, but we can make a better estimate of depth extent once we have measured density values to provide constraints on the density contrast. The outer arcuate bodies which play a prominent role in matching the magnetic anomaly appear to have no expression in the gravity field, and are believed to be of a less dense (probably less basic) lithology, suggesting that this complex may be a fractionated system.

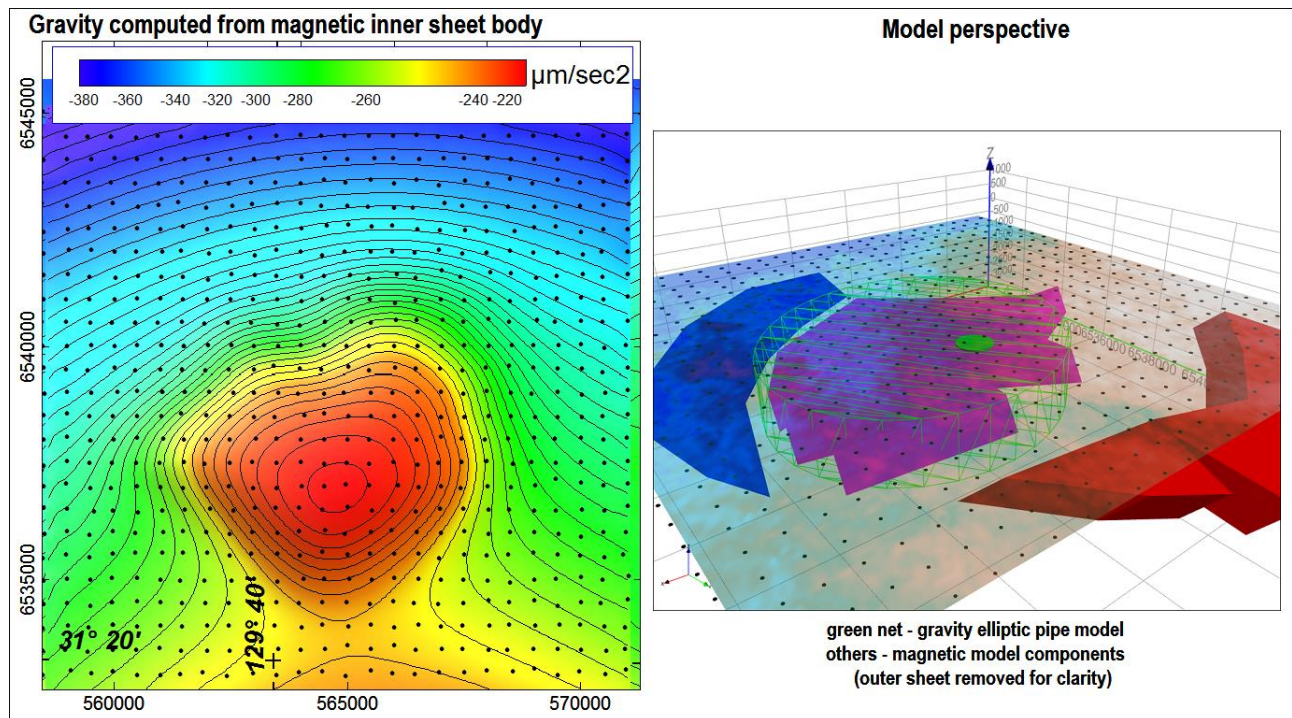


Figure 12 (left) Computed gravity from the central sheet magnetic inversion model, and (right) the elliptic sheet gravity inversion model together with the magnetic field inversion model (with the outer sheet component removed).

CONCLUSIONS

Initial inversions of discrete anomalies in new gravity and magnetic data over the Coompana area have provided separate mappings of density and (predominantly remanent) magnetization. Drilling results have confirmed interpretation of these high density, high remanent magnetization bodies as being due to gabbroic material. Individually the gravity and magnetic bodies can mostly be well explained with simple, homogeneous property sources, but in some cases discrepancies between the gravity and magnetization models reveal that at least one of the property distributions must be complex, and that there is not a constant relationship between the two properties. In this way the combined gravity and magnetic surveys provide more information than is available from either separately. We hope to advance these subsurface models further once we can incorporate physical property measurements from the recent drilling, and from petrological studies can understand the geological controls on the physical properties and use that understanding to build more interpretive geological models from these initial geophysical inversions. We hope also to relate the results between sources of the different anomalies to understand the complete geological system, its relation to the (as yet still unexplained) major magnetic and gravity anomaly, and speculate on possible mineralisation.

ACKNOWLEDGMENTS

The South Australian Government PACE Copper Initiative is acknowledged for funding this project.

REFERENCES

Foss, C., Reed, G., Keeping, T., Wise, T., and Dutch, R., 2016. Inversion of an anomaly due to multiple magnetizations: An example from the Coompana survey, South Australia. SEG Technical Program Expanded Abstracts 2016: pp. 1511-1515. <https://doi.org/10.1190/segam2016-13972845.1>

Wise, T., Pawley, M.J., Dutch, R., 2015. Preliminary interpretations from the 2015 Coompana aeromagnetic survey. MESA 79 (4), 22-30.